PHYSICAL REVIEW B VOLUME 61, NUMBER 4 15 JANUARY 2000-II

Polariton-polariton scattering in semiconductor microcavities: Experimental observation of thresholdlike density dependence

T. Baars, M. Bayer, A. Forchel, F. Schäfer, and J. P. Reithmaier
Technische Physik, Universität Würzburg, Am Hubland, 97074 Würzburg, Germany

(Received 19 February 1999; revised manuscript received 24 September 1999)

Polariton-polariton scattering in semiconductor microcavities has been studied by time-integrated, degenerate four-wave mixing using spectrally compressed pulses. We find a thresholdlike behavior for the density dependence of the scattering rate γ in the lower polariton branch. At low densities scattering is suppressed due to the small density of final states for the scattering process. At higher density γ increases as excitonlike states become accessible for the scattering and the scattering strength only depends on the exciton fraction of the initial states. The threshold density depends on the detuning between the polariton branches. The experimental findings are in qualitative agreement with calculations using the self-consistent Born approximation.

Semiconductor microcavities (MC's) provide an interesting system to study light-matter interactions in solids.[1,2] The coupling strength between the electromagnetic field and the electronic excitations can be controlled by the design of the structure. In the so-called strong-coupling regime the confined optical modes and the excitons form new eigenstates that are termed cavity polaritons. The minimal splitting between these modes, the so-called Rabi splitting, is a measure of the coupling strength between exciton and photon. Cavity polaritons have been investigated heavily in the past few years using linear spectroscopic techniques such as reflection, transmission, and photoluminescence in both cw and time-resolved studies.[3,4]

More recently polariton scattering phenomena in MC's have attracted particular attention. Large differences in the scattering properties of cavity polaritons as compared to, e.g., excitons in quantum wells can be expected because the dispersion relations of the polaritons are very different from those of bare excitons in quantum wells due to the small polariton mass ($m \approx 10^{-5} m_e$). Various spectroscopic techniques including resonant Raman scattering,[5] four-wave mixing (FWM),[6–8] and coherent control experiments[9] have been employed to study different scattering mechanisms such as disorder scattering,[10] scattering of polaritons by phonons, and polariton-polariton scattering. The experiments revealed significant differences between the scattering processes in the lower (LPB) and upper (UPB) polariton branch. For example, Marie *et al.* have found that acoustic phonon scattering in the LPB is suppressed up to a temperature where scattering into the excitonic region of the LPB dispersion curve becomes possible.[9] Baumberg *et al.* have shown that most scattering mechanisms are inhibited in the LPB resulting in a strong suppression of the LPB scattering as compared to the UPB.[11]

Although many aspects of polariton scattering have already been investigated there is still a lack of detailed experimental studies addressing the role of exciton-exciton interaction as a possible scattering mechanism in MC's. However, in a recent work polariton scattering due to exciton-exciton interaction has been investigated theoretically. This theory predicts a threshold behavior of the homogeneous broadening of the lower polariton branch as the polariton density is increased.[12]

In this work we have systematically investigated polariton-polariton scattering using density-dependent, time-integrated four-wave mixing (TI-FWM). TI-FWM is a well-suited technique for the study of scattering processes in semiconductor structures. Previously density-dependent FWM has been successfully applied to the study of exciton-exciton scattering in low-dimensional semiconductors such as quantum wells[13] and quantum wires.[14]

Using spectrally tailored pulses we were able to study selectively the polariton scattering in either the lower or upper polariton branch. For the UPB we find a fast dephasing that is attributed to the effective scattering into excitonic states with a large in-plane wave vector. For the LPB we can clearly distinguish two regimes of the density dependence of the dephasing rate: Below a certain polariton density scattering is reduced due to the small density of states of lower branch polaritons. Above this density scattering into exciton-like states is possible and the scattering strength increases. Both the density at which the two regimes cross over and the scattering strength depend on the excitonic fraction of the initial scattering states.

The MC investigated in this work contains a single 7-nm-wide $In_xGa_{1-x}As$ ($x=0.14$) quantum well at the antinode of a λ GaAs cavity. The top (bottom) mirror consists of 21 (23) pairs of distributed Bragg reflectors with a reflectivity of 99.5%. The wedgelike shape of the sample permitted the variation of the detuning $\Delta = E_c - E_e$ between the cavity mode and the heavy-hole exciton mode by changing the position of the laser spot on the sample.

Degenerate FWM experiments were performed in the two-pulse self-diffracting transmission geometry[15] using a fs mode-locked Ti:sapphire laser. In this configuration two short pulses having wave vectors $\mathbf{k}_1$ and $\mathbf{k}_2$ are focused onto the same spot on the sample at a small angle and the FWM signal is emitted in the direction $2\mathbf{k}_2$-$\mathbf{k}_1$. In our experiments the pulses were collinearly polarized. The FWM signal is spectrally resolved by a monochromator and detected by a charge-coupled device camera as a function of photon energy E and delay τ between the two pulses.

To excite the polariton branches separately the short pulses provided by the fs laser were spectrally compressed to

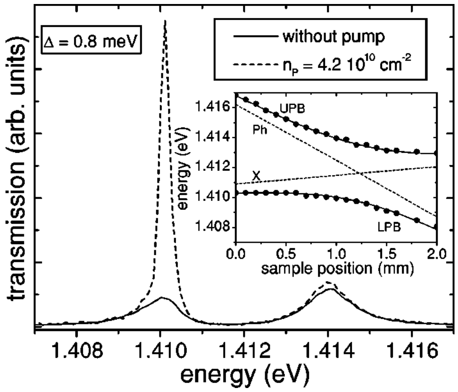

FIG. 1. Pump-probe transmission spectra without an additional population of the LPB (full line) and with a population of $n_P \approx 4.2\times10^{10}$ cm^{-2} (dashed line). The inset shows the spectral positions of the two cavity modes as a function of the sample position. The full lines represent model calculations as explained in the text. The dotted lines are the calculated energies of the uncoupled exciton and photon modes.

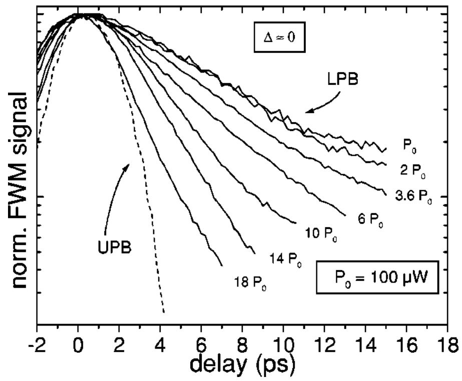

FIG. 2. Decay of the FWM signal as a function of the delay between the pulses for resonant excitation of LPB (full lines) and UPB (dashed lines).

a width of ~1.6 meV using a grating and a slit. Transmission experiments have been performed using the spectrally broad fs pulses as a light source. In all experiments the sample was kept in superfluid helium at a temperature of 2 K.

Figure 1 shows the transmission spectrum (full line) of the microcavity sample close to resonance. The two polariton modes can be well resolved, because the Rabi splitting of $\Omega=3.8$ meV is significantly larger than the linewidths of the two modes (FWHM=1.0 meV for the LPB and 1.2 meV for the UPB, respectively). The two cavity polariton modes show a clear anticrossing as the position of the laser spot is varied across the sample, as shown in the inset of Fig. 1. We have fitted the experimental data using a standard coupled two-level exciton-photon model (solid lines in inset).[16] In the model the cavity polariton wave function is written as a linear combination of the exciton and photon wave functions ($|X\rangle$ and $|C\rangle$, respectively): $|P\rangle=\alpha_X|X\rangle+\alpha_C|C\rangle$. The uncoupled photon and exciton energies (dotted lines in inset) and the Hopfield coefficients (α_X and α_C) that give the exciton and photon fractions of the mixed-particle states, respectively, were calculated from the spectral positions of the polariton modes.

To ensure that under the excitation conditions used in the FWM experiments the strong-coupling regime is preserved, we also monitored the transmission of a weak broadband probe beam while a population of lower branch polaritons was excited by a resonant pump beam. Even for the highest polariton densities used in the FWM experiments we clearly observe the two polariton branches with no significant shift of the spectral lines as shown in the probe transmission spectrum (dashed line) in Fig. 1 for an excitation of $n_P \approx 4.2\times10^{10}$ cm^{-2} polaritons in the LPB.[17]

The decay of the TI-FWM signal at a detuning of $\Delta\approx0$ as a function of the delay between the pulses is shown in Fig. 2. When only the UPB is excited (dashed line) the TI-FWM signal decays rapidly, independent of the cavity detuning, and a comparison with the autocorrelation signal of the two exciting pulses shows that the decay of the FWM signal in this case is limited by the length of the exciting compressed pulses even for the lowest excitation intensities used in the experiment. When only the LPB is excited (full lines) the TI-FWM signal shows a nearly exponential decay that strongly depends on the excitation intensity at higher excitation. The decay time, which is inversely proportional to the homogeneous linewidth for dominantly homogeneously broadened microcavity samples,[8,18] is obtained from exponential fits to the data at longer delay times. It decreases from $\tau_D^{LPB}\approx6.9$ ps for an incident power of $P_0=100$ μW to $\tau_D^{LPB}\approx1.8$ ps for $P=18P_0$. However, as can be seen from the figure, the decay time shows only a weak intensity dependence at low excitation intensities.

The differences in the decay of the FWM signal may be explained by the different scattering channels accessible for the polaritons. The incident laser pulses create polaritons in the MC with well-defined in-plane wave vectors that can be calculated from the angle of incidence. Subsequently, two polaritons with wave vectors $(\mathbf{k}_0,\mathbf{k}_0')$ $(|\mathbf{k}_0|=|\mathbf{k}_0'|\approx5\times10^5$ m^{-1} in our experiments) can be scattered into different states having wave vectors $(\mathbf{k},\mathbf{k}')$. If the LPB is excited resonantly these final states are limited to the lower branch. As will be discussed below this intraband scattering depends characteristically on the polariton density and the exciton fraction of the lower branch polaritons. In constrast, polaritons that are selectively excited in the UPB can scatter into final states both on the UPB and the LPB. Scattering into excitonlike states with large $|\mathbf{k}|$ on the LPB dispersion curve is strongly favored in this case because the density of these states is much larger than the density of coupled polariton states. This effective scattering mechanism leads to the faster dephasing of the UPB as compared to the LPB. In the following we shall focus on the detuning dependence and the excitation density dependence of the TI-FWM decay rate for selective excitation of the LPB. The excitation density n_P has been calculated from the absorbed average power density P_a, which we deduced from the incident intensity P_i by $P_a=AP_i$. The absorption A has been obtained directly from reflectivity measurements by $A=1-R$, where R is the reflectivity at the energy of the lower polariton branch. The transmission T has been neglected here because in the experiment it was a factor of $\lesssim10^{-2}$ smaller than R.

Figure 3 shows the decay rate $\gamma=1/\tau_D^{LPB}$ as a function of the polariton density for different detunings.[19] Note that for clarity we have subtracted a constant, density-independent value $\gamma_0\approx0.1$ ps^{-1}. Two different density regimes display-

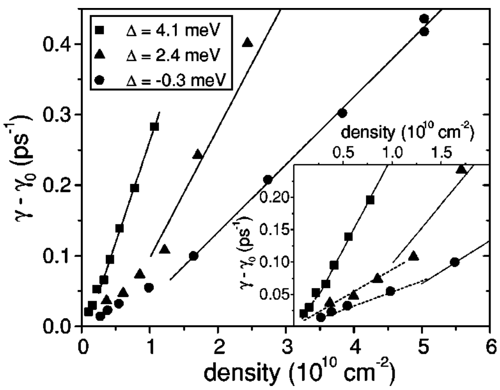

FIG. 3. Decay rate of the FWM signal for resonant excitation of the LPB as a function of polariton density for $\Delta=-0.3$, 2.4, and 4.1 meV corresponding to an excitonic admixture of $|\alpha_X|^2\approx 0.5$, 0.8, and 0.9. The symbols correspond to the experimental data; the full lines are linear fits. The inset shows a closeup of the main figure for small polariton densities. The lines are again linear fits.

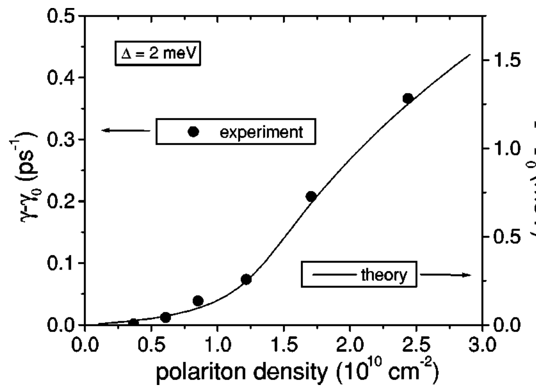

FIG. 4. Experimental FWM decay rates (dots, left axis) and calculated scattering broadening (full line, right axis) as a function of polariton density for a detuning of $\Delta\approx 2$ meV.

ing a thresholdlike changeover can clearly be distinguished. In both regimes the decay rate is approximately proportional to the density as indicated by the lines that are linear fits to the experimental data. However, in the low-density regime the slope that is a measure of the scattering strength is significantly smaller than in the high-density regime. The slope increases with increasing detuning or, which is equivalent, increasing exciton fraction of the lower polariton branch. At the same time the threshold density at which the crossover between the two regimes occurs decreases from 1.4×10^{10} cm^{-2} at $\Delta\approx 0$ to 0.3×10^{10} cm^{-2} at $\Delta\approx 4$ meV. These threshold densities are below the saturation density of the strong-coupling regime reported in the literature.[20,21] Thus the change in the scattering strength is not related to the onset of the weak-coupling regime. As discussed above we can clearly observe the coupled modes in the spectra even at these polariton densities. It should also be noted that the saturation densities given in the literature have been obtained for nonresonant excitation conditions. In that case the strong coupling is destroyed already at moderate densities due to efficient scattering with free carriers.[21]

The density dependence of the decay rate can be written as

$$\gamma(n_P)=\gamma_0+\gamma_{PP}n_P, \tag{1}$$

where γ_0 is the density-independent part of the decay rate and the scattering parameter[12]

$$\gamma_{PP}\propto\sum_{k,k'}|\langle P_kP_{k'}|V|P_{k_0}P_{k_0}\rangle|^2 \times\frac{2\gamma}{[E(k)+E(k')-2E(k_0)]^2+4\gamma^2} \tag{2}$$

describes the strength of the polariton-polariton scattering. The polariton-polariton scattering is due to the Coulomb interaction, in particular to the interexciton exchange,[14,22] which only acts on the excitonic parts of the cavity polaritons. Thus, the matrix element in Eq. (2) can be reduced to

$$|\langle P_kP_{k'}|V|P_{k_0}P_{k_0}\rangle|^2=|\alpha_X^{k_0}|^4|\alpha_X^k|^2|\alpha_X^{k'}|^2|\langle X_kX_{k'}|V|X_{k_0}X_{k_0}\rangle|^2 \tag{3}$$

with $|P_k\rangle=\alpha_X^k|X_k\rangle+\alpha_C^k|C_k\rangle$. Note that the scattering parameter in Eq. (2) contains an implicit density dependence. Thus the polariton-polariton scattering increases with increasing width of the Lorentzian γ. At low densities γ is small, therefore only scattering within the polaritonic part of the LPB dispersion relation is allowed. The small density of states in this region results in a small scattering strength. As the polariton density is increased the Lorentzian gets smeared out. When the scattering broadening becomes comparable to the width of the lower polariton band, ΔE_{LPB} final states with large $|\mathbf{k}|$ become accessible by the scattering process, and the scattering strength increases due to the large density of states in the excitonic part of the dispersion curve and the larger exciton fractions of the final states. As ΔE_{LPB} decreases when the LPB dispersion becomes more and more excitonic, the treshold density is reduced with increasing detuning. At the same time the scattering strength in the low-density regime increases. It has recently been shown theoretically that the scattering broadening in the LPB is reduced by as much as a factor of the order of the inverse polariton mass for an ideal MC with negligible density-independent broadening.[12] However, in real structures the finite magnitude of the

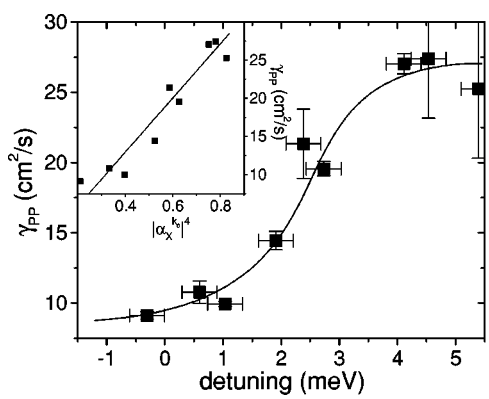

FIG. 5. LPB scattering parameter γ_{PP} vs cavity detuning. The inset shows the scattering parameter vs the square of the exciton fraction of the initial scattering states $|\alpha_X^{k_0}|^4$. The lines are guides to the eye.

density-independent part of the homogeneous linewidth leads to a significant increase of the scattering in the low-density regime and a softening of the threshold. We have solved Eq. (2) numerically using γ_0 as obtained from the experiment. As can be seen in Fig. 4 there is a reasonable qualitative agreement between the calculated homogeneous linewidth and the experimental scattering rates. In particular the threshold density and the relative slopes in the two regimes are well reproduced in the model. However, there is a significant difference in the absolute magnitude of the scattering broadening that is most likely related to the assumption made in the model of an ideal two-dimensional confinement disregarding localization due to disorder.[22]

Above the threshold density the scattering strength γ_{PP} is still reduced by the detuning-dependent exitonic admixture $|\alpha_X^{k_0}|^4<1$ of the initial states. The detuning dependence of γ_{PP} as obtained from a linear fit to the density-dependent decay rates is shown in Fig. 5. In the excitonic limit ($\Delta \to \infty$, $|\alpha_X^{k_0}|^4 \to 1$) the scattering strength approaches a constant value of $\gamma_{PP} \approx 27\ \mathrm{cm}^2/\mathrm{s}$. This value agrees very well with the scattering strength of bare excitons reported in the literature.[13,14] The inset of Fig. 5 shows γ_{PP} plotted vs $|\alpha_X^{k_0}|^4$ from which an approximately linear relation can be seen. Thus, in the high-density limit the final states do not influence the polariton scattering strength significantly.

We gratefully acknowledge fruitful discussions with C. Ciuti and his critical reading of the manuscript. This work has been supported financially by the Deutsche Forschungsgemeinschaft and the State of Bavaria.

[1] C. Weisbuch, M. Nishioka, A. Ishikawa, and Y. Arakawa, Phys. Rev. Lett. **69**, 3314 (1992).

[2] R. Houdré *et al.*, Phys. Rev. Lett. **73**, 2043 (1994).

[3] For a recent review see, e.g., M.S. Skolnick, T.A. Fisher, and D.M. Whittaker, Semicond. Sci. Technol. **13**, 645 (1998).

[4] See, e.g., *Confined Electrons and Photons, New Physics and Applications*, Vol. 340 of NATO Advanced Study Institute, Series B: Physics, edited by E. Burstein and C. Weisbuch (Plenum, New York, 1995).

[5] W.R. Tribe *et al.*, Phys. Rev. B **56**, 12 429 (1997).

[6] H. Wang *et al.*, Phys. Rev. B **51**, 14 713 (1995).

[7] M. Kuwata-Gonokami *et al.*, Phys. Rev. Lett. **79**, 1341 (1997); M. Shirane *et al.*, Phys. Rev. B **58**, 7978 (1998).

[8] G. Bongiovanni *et al.*, Phys. Rev. B **55**, 7084 (1997).

[9] X. Marie *et al.*, Phys. Rev. B **59**, R2494 (1999).

[10] D.M. Whittaker *et al.*, Phys. Rev. Lett. **77**, 4792 (1996); D. M. Whittaker, *ibid.* **80**, 4791 (1998).

[11] J.J. Baumberg, A. Armitage, M.S. Skolnick, and J.S. Roberts, Phys. Rev. Lett. **81**, 661 (1998).

[12] C. Ciuti *et al.*, Phys. Rev. B **58**, R10 123 (1998).

[13] A. Honold, L. Schultheis, J. Kuhl, and C.W. Tu, Phys. Rev. B **40**, 6442 (1989).

[14] W. Braun *et al.*, Phys. Rev. B **57**, 12 364 (1998).

[15] See, e.g., J. Shah, *Ultrafast Spectroscopy of Semiconductors and Semiconductor Nanostructures* (Springer-Verlag, Berlin, 1996).

[16] See, e.g., B. Sermage *et al.*, Phys. Rev. B **53**, 16 516 (1996).

[17] The origin of the nonlinearity responsible for the enhanced transmission at the position of the LPB is not completely clear yet. However, it is not related to excitonic bleaching because it leaves the Rabi splitting unchanged.

[18] Following Ref. 8 we conclude from the appearance of pronounced quantum beats between the polariton modes in FWM experiments with broadband excitation that for the present sample the FWM decay rate can be taken as proportional to the homogeneous broadening.

[19] We found that the transmission cannot be neglected for negative detunings introducing large experimental uncertainties to the calculation of the excitation density. Thus, we do not show experimental data for $\Delta<0$. However we note that we did not observe a thresholdlike density dependence in this case.

[20] R. Houdré *et al.*, Phys. Rev. B **52**, 7810 (1995).

[21] F. Jahnke *et al.*, Phys. Rev. Lett. **77**, 5257 (1996).

[22] C. Ciuti *et al.*, Phys. Rev. B **58**, 7926 (1998).